Question 1

The paper examines human hand impedance characteristics which include inertia, viscosity and the stiffness in multi joint arm movements. Hand impedance is estimated by measuring hand displacements and forces caused by external disturbances. The inertia, viscosity and stiffness are estimated using a second order linear model. The accuracy of the estimation was validated using a mass spring damper system with known parameters. The estimated inertia matrices in different subjects of the human hand agrees with the computed values of a two joint arm model, the spatial variations of the stiffness ellipses are consistent with the experimental results of Mussa Ivaldi. The hand stiffness and the viscosity increase with the force used to grip and varies for each subject. The viscosity and the stiffness ellipses have similar orientation. The sampling interval of the controller used for the experiment was 0.65ms. The force vector between the hand and the handle was measured by a force sensor attached to the handle of the robot. The arm posture of the subject was measured by a stereo-PSD camera system. The data sampling intervals were 1ms for hand force and positions and 10ms for 3D arm postures. The attention was focused on hand manipulation linkage.

Observations and Findings:

- The paper focuses on understanding the impedance characteristics of the hand which is crucial for various applications.
- The paper provides insights into the biomechanical properties of the hand
- By mimicking the impedance characteristics of the hand the devices achieve greater stability and dexterity
- Hand impedance varies over time during maintained posture

The control hypothesis theory assumes that the actual trajectory of the arm is affected by the gradual change in torque and the impedance is controlled by the viscoelastic properties of the muscle. The central nervous system helps in maintaining the musculoskeletal system without decoding the dynamic problem. This static model mainly administers arm stiffness and plays an important role in reimbursing the non-linear dynamics of arm moment. This static model mainly administers arm stiffness and plays an important role in reimbursing the non-linear dynamics of arm moment. Based on the stiffness of the hand obtained during the transfer of forces, it was found that the stiffness of the hand depends on the position of the hand and the position in the horizontal plane. Before the experiment, it is important to determine the role of hand viscosity in multi-joint movements, because the viscous properties of muscles vary greatly according to their activation levels. Voluntary muscle activation was the cause of joint slumping. This explained the increase in the size of the ellipse from the activation of its muscles. This muscle activation is due to the movement of the elbow and hand of the grip forces holding the handle. The approximate inertia of the human hand followed or accepted the calculated values of the 2-joint motion model. The grip strength of the patient increases the stiffness and viscosity of the hand. The direction of the viscosity ellipse is parallel to the stiffness ellipse.

Question 2

Cyberknife robotic technology system utilizes a combination of robotics and image guidance to treat tumors. It involves the use of computer software to design and plan surgical procedures, CAM translates the designs into precise actions during the operation. CAD is employed to plan the trajectory and dosage of radiation beams to target tumors. The process begins with imaging techniques which generate detailed 3D models of the anatomy. Surgeons use software to delineate the tumor and the surrounding structures. The software calculates optimal treatment paths, taking into account of dynamic movements of organs. The CyberKnife System features a linear accelerator directly mounted on a robot to deliver the high-energy x-rays or photons used in radiation therapy. The robot moves and bends around the patient, to deliver radiation doses from different beam angles, expanding the possible positions to concentrate radiation to the tumor while minimizing dose to surrounding healthy tissue. During treatment Cyberknife dynamically adjusts the radiation delivery based on the tumor's position and movement. The challenge of lung tumors is addressed by cyberknife technology by employing motion tracking and compensation mechanisms. Real time imaging, such as fluoroscopy or respiratory gating, is utilized to monitor lung movement during treatment. The system adjusts the radiation beams accordingly, ensuring precise targeting even as the tumor and surrounding tissues move. The benefits of adopting the cyberknife technology includes –

- CyberKnife's submillimeter accuracy allows for highly targeted radiation delivery, minimizing damage to healthy tissues and reducing side effects.
- CyberKnife treatment is non-invasive, eliminating the need for incisions and reducing recovery times.
- The system can treat tumors in various locations throughout the body, including those in challenging or hard-to-reach areas.
- The ability to track organ motion and adjust treatment in real-time enhances safety and efficacy, particularly in moving organs like the lung.

The technology has been used to treat brain, spine, liver, prostate, and pancreatic tumors. Its versatility and precision make it particularly effective for tumors located near critical structures or in areas where conventional surgery may be risky. Traditional radiotherapy requires multiple sessions, whereas CyberKnife can often achieve similar outcomes in fewer sessions, reducing treatment duration and improving patient convenience. The precise targeting capabilities of CyberKnife minimize radiation exposure to healthy tissues.

Cyberknife technology can be improved by enhancing the imaging technology to visualize tumors and surrounding structures, compensation algorithms could further improve the system's ability to treat tumors in moving organs and automation of treatment planning and delivery processes could streamline workflow, reducing treatment times and increasing efficiency.

Question 3

Designed for user manipulation during patient procedures, it integrates a haptic device for tactile feedback. This allows the user to interact with precision, aided by the computer's control parameters based on patient anatomy and device dynamics. This setup ensures haptic control and adjusts parameters in response to anatomical movements. The seamless integration with haptic devices provides real-time feedback to the operator. The users interact with the system guided by the control parameters. The system ensures haptic control and adaptability to the patients' movements during the procedure.

Minimally invasive surgery (MIS) features notably smaller incisions compared to traditional methods, benefiting orthopedic applications like total knee replacement. While MIS reduces soft tissue trauma, hastens recovery, and minimizes discomfort, its limitation lies in restricted visibility for surgeons. Achieving precise outcomes requires significant skill. Traditional robotic systems assist in surgery, primarily aiding in bone preparation or collaborating with surgeons. However, these systems lack real-time adaptability during procedures.

The surgical method involves creating a representation of the patient's anatomy, associating images with surgical instruments, and adapting hardware accordingly. Before surgery, a CT scan generates a 3D model of the joint, aiding in bone structure analysis. During the procedure, the surgical device offers either haptic guidance or limit manipulation of the device. Joint replacement method entails bone preparation by image of the first and second bones and implant placement planning. the first bone is prepared to receive the first implant by manipulating the surgical tool to shape the first bone, and then bone preparation is planned to place the second implant in the second bone after the first bone is ready. A surgical tool is used to shape the second bone to prepare the second implant, this prepares the second bone to receive the implant. Surgical planning includes determining cartilage height and bone preparation this creates an image of the height of the cartilage in addition to the bone, and plans the preparation of the bone to implant the implant into the bone.

The computer system is pivotal, facilitating surgical planning, navigation, and image and haptic guidance. Surgical planning, navigation, and basic image-based surgical functions are available through computer-assisted surgery utilities. Functions to generate and display images from image data series, determine the position and axis direction of the surgical instrument tip, and register the patient and image data set in the tracking system. Application programs cater to various medical procedures, including orthopedic surgeries. Target position information is conditioned using interpolation filters which refines target position information for precise control in the cases where the tracking system operates at a lower frequency than haptic control procedures This filter smoothes object position information by filling the gaps between discrete data samples, allowing it to be used in higher-frequency haptic control procedures. This approach combines technology and surgical expertise for optimal patient outcomes.

Question 4

Concentric Tube Robotics (CTR) is an emerging field in surgical robotics that utilizes a system of concentrically arranged tubes to perform minimally invasive procedures with enhanced dexterity and precision. These robots consist of multiple flexible tubes, mimicking the structure of a catheter. They are typically made of elastic pre-curved tubes nested one inside the other. Translation and relative rotation of the tubes at their base make them bend and twist, resulting in a needle-size robot. The elastic interaction between the tubes provides the steering force, therefore, CTRs have been used as steerable needles. CTRs steer without depending on the tissue interaction force allowing them to navigate in hollow or liquid filled cavities.

Benefits of CTRs:

- CTRs enable surgeons to perform minimally invasive surgeries, allowing intricate procedures to be performed through small incisions.
- The flexible nature of concentric tubes allows for precise navigation through complex anatomical structures, enhancing surgical dexterity and maneuverability.
- CTR systems are adaptable to various surgical specialties.
- Integration of advanced imaging modalities enhances visualization.

The highly flexible nature of concentric tubes poses challenges in controlling their motion accurately within the surgical site, fabricating concentric tubes with precise mechanical properties is also a challenge. CTR has been deployed in neurosurgery due to the need for dexterous devices with enhanced controllability with minimal risk of collateral damage. They are also used in treatment of lung cancer, cardiac catheters are used for suturing, tissue ablation, and the delivery of drugs and implants. They are also used in gastric, prostate, kidney, larynx, eye and fetal surgeries.

Interaction between the environment and the robotic backbone causes deformation, resulting in singularities and rendering the model-based control unreliable. Concentric tubes exhibit elastic instability, small perturbations in the system's configuration leads to changes in the tubes' shape. This instability affects the predictability and controllability of the robotic system during surgical maneuvers. The sudden branching of the motion trajectories occurs due to non-linearities in the system dynamics leading to unpredictable behavior of the CTR.

References:

1. Okamura, Allison M., Jessica Burgner-Kahrs, and Robert J. Webster III. "Soft robotics: new perspectives for robot-assisted surgery." International Journal of Robotics Research
2. Rucker, Daniel C., et al. "A review of concentric tube robots: from fundamentals to medical applications." IEEE Transactions on Robotics
3. Bruns TL, Remirez AA, Emerson MA, et al. A modular, multi-arm concentric tube robot system with application to transnasal surgery for orbital tumors. The International Journal of Robotics Research.

4. H. Alfalahi, F. Renda and C. Stefanini, "Concentric Tube Robots for Minimally Invasive Surgery: Current Applications and Future Opportunities," in IEEE Transactions on Medical Robotics and Bionics
5. Alfalahi, Hessa & Renda, Federico & Stefanini, Cesare. Concentric Tube Robots for Minimally Invasive Surgery: Current Applications and Future Opportunities. IEEE Transactions on Medical Robotics and Bionics

Question 5

```
%Define constants
clear;
dt = 0.001; % time step
T = 120; %total time in s
N = 50; % number of dominant frequency components
F0 = 1; %starting frequency rad/s
df = 1; %frequency step
mu = 0.01; %adaptive gain parameter
%variables
omega = zeros(1, N+1); % array of frequencies
phi_mp = zeros(2, N+1); %reference input,1st row sin 2nd row cos
theta_mp = zeros(2,N+1); %weights, 1st row sin 2nd row cos
%reference signal
t = zeros(1, T/dt);
omega=F0:df:F0+N;
t=0:dt:T-dt;
s =sin(t)+2*sin(2*t)+3*sin(3*t)+0.1*sin(30*t)+0.1*sin(35*t)+cos(t)+2*cos(2*t)+3*cos(3*t)+0.1*cos(30*t)+0.1*cos(35*t);
y_mp=zeros(1,length(t));

for i=1:length(t)
phi_mp(1,:)=sin(omega*t(i));
phi_mp(2,:)=cos(omega*t(i));
    for k=1:N+1
       y_mp(i) = y_mp(i) + theta_mp(1,k)*phi_mp(1,k)+theta_mp(2,k)*phi_mp(2,k);
       err = s(i) - y_mp(i);
       theta_mp(1,k) = theta_mp(1,k) +2*mu*phi_mp(1,k)*err;
       theta_mp(2,k) = theta_mp(2,k) +2*mu*phi_mp(2,k)*err;
    end
end
Mp=s;
plot(t,Mp,'LineWidth',2,'Color','b');
hold on;
plot(t,y_mp,'LineWidth',1,'Color','r'); %estimate of total signal
legend('M\_p','Signal estimate');
N = 3; % truncated number
%variables
Mpv = sin(t)+2*sin(2*t)+3*sin(3*t)+cos(t)+2*cos(2*t)+3*cos(3*t);
s=Mpv;
omega_v=F0:df:F0+N;
phi_mpv = zeros(2, N+1); %reference input,1st row sin 2nd row cos
theta_mpv = zeros(2,N+1); %weights, 1st row sin 3nd row cos
```

```
y_mpv=zeros(1,length(t));
for i=1:length(t)
phi_mpv(1,:)=sin(omega_v*t(i));
phi_mpv(2,:)=cos(omega_v*t(i));

    for k=1:N
       y_mpv(i) = y_mpv(i) + theta_mpv(1,k)*phi_mpv(1,k)+theta_mpv(2,k)*phi_mpv(2,k);
       err = s(i) - y_mpv(i);
       theta_mpv(1,k) = theta_mpv(1,k) +2*mu*phi_mpv(1,k)*err;
       theta_mpv(2,k) = theta_mpv(2,k) +2*mu*phi_mpv(2,k)*err;
    end
end
figure;
plot(t,Mpv,'LineWidth',2,'Color','b'); %real voluntary movement signal
hold on;
plot(t,y_mpv,'LineWidth',1,'Color','r'); %voluntary movement estimate
legend('M\_pv','Voluntary signal estimate');
```

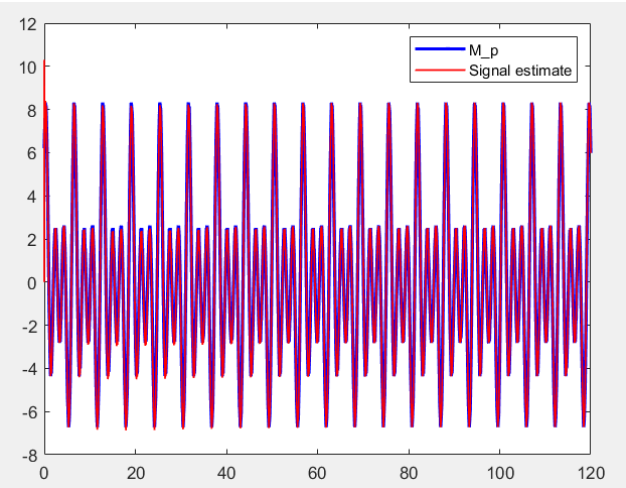

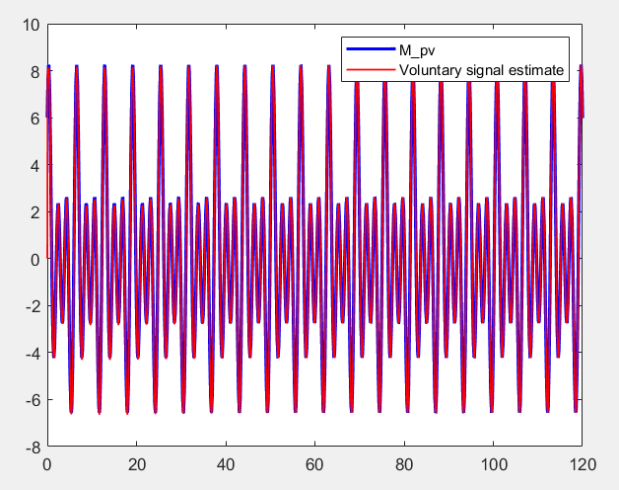

- Yes, the estimated signal follows the main signal according to the graph.

- The estimated Mpv signal closely matches the main Mpv signal in terms of amplitude, indicating that the BMFLC filter is effective in estimating the desired signal.
- The results are consistent with the expectation that the BMFLC filter can separate the voluntary component from the tremor component and thus can be useful for tremor filtering.
- There is no need for forgetting factor as the frequencies are constant

Question 6

- The given system is not a linear system.
- Subsystem 1:

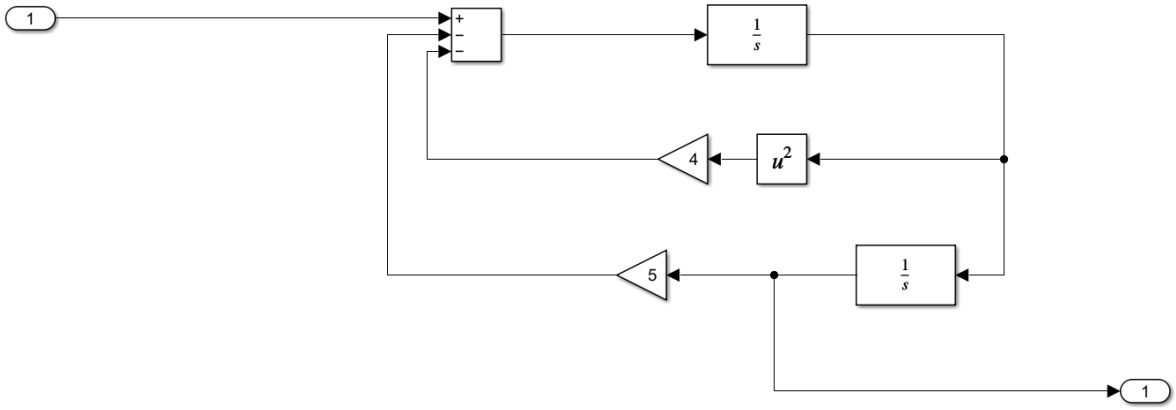

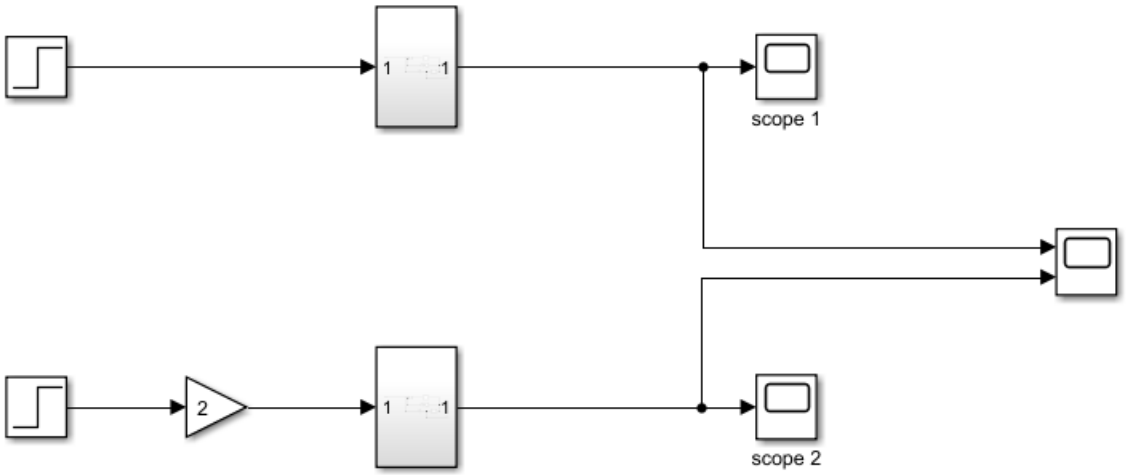

u(t) = 1

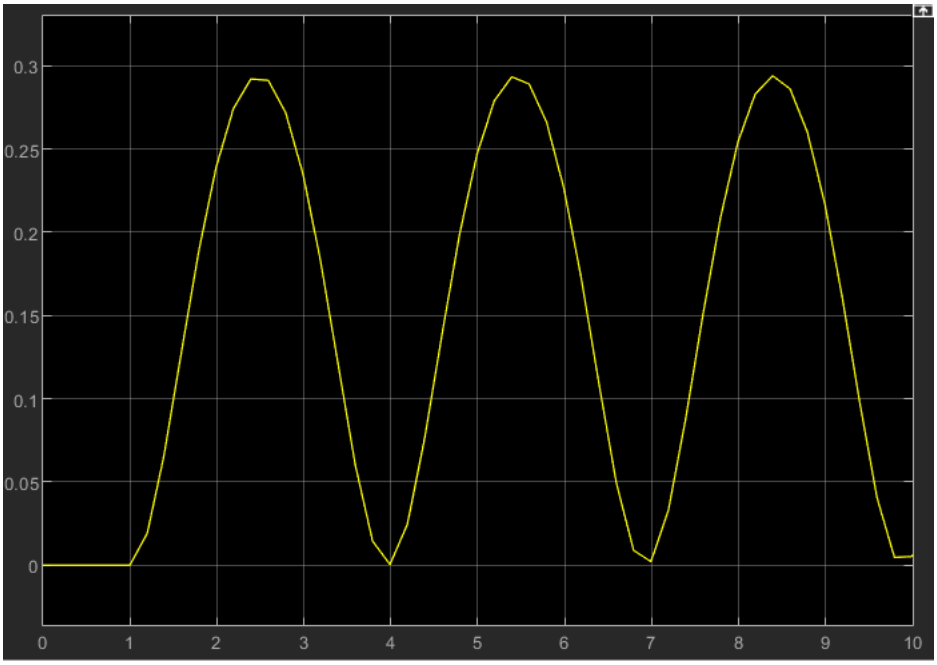

u(t) = 1 with amplification 2

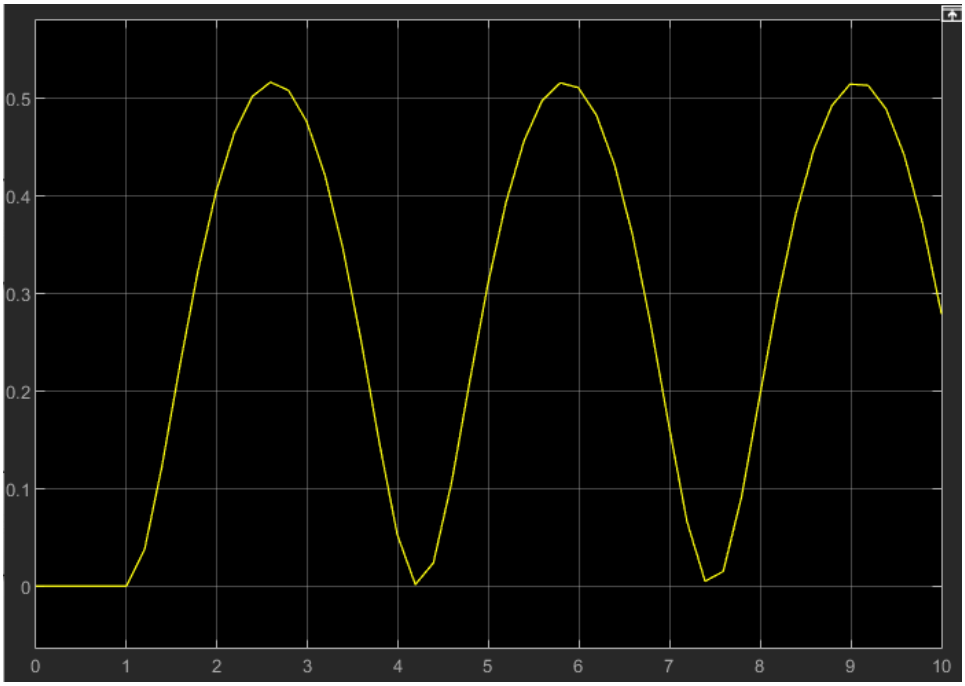

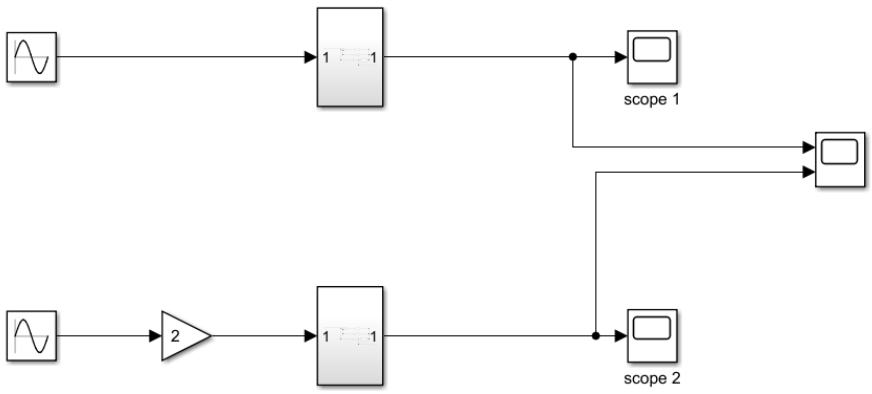

u(t) = sin(3t)

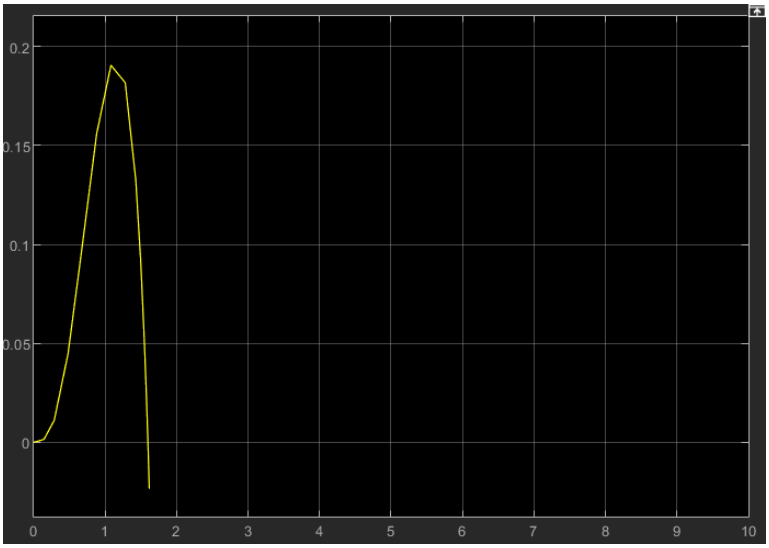

u(t) = sin(3t) with amplification of 2

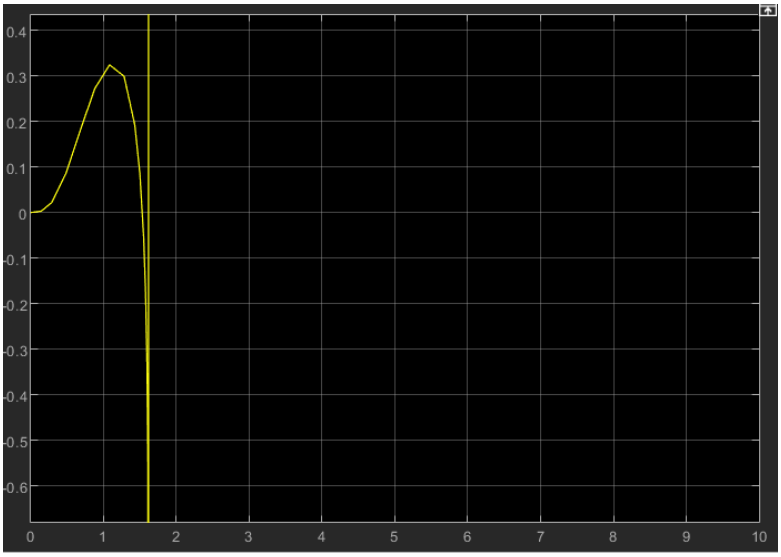

- The outputs of the system are not amplified by 2 they are amplified by a factor close to 1.75
- The system with constant input is stable
- The system with sine input is not stable and diverges
- $\dot{x}_2(t) = -5x_1(t) - 4x_2^2(t) + u_c(t)$

  $u_c(t) = 10F_e(t) - 0.1\dot{x}_1(t) - x(t) + 5x_1(t) + 4x_2^2(t)$

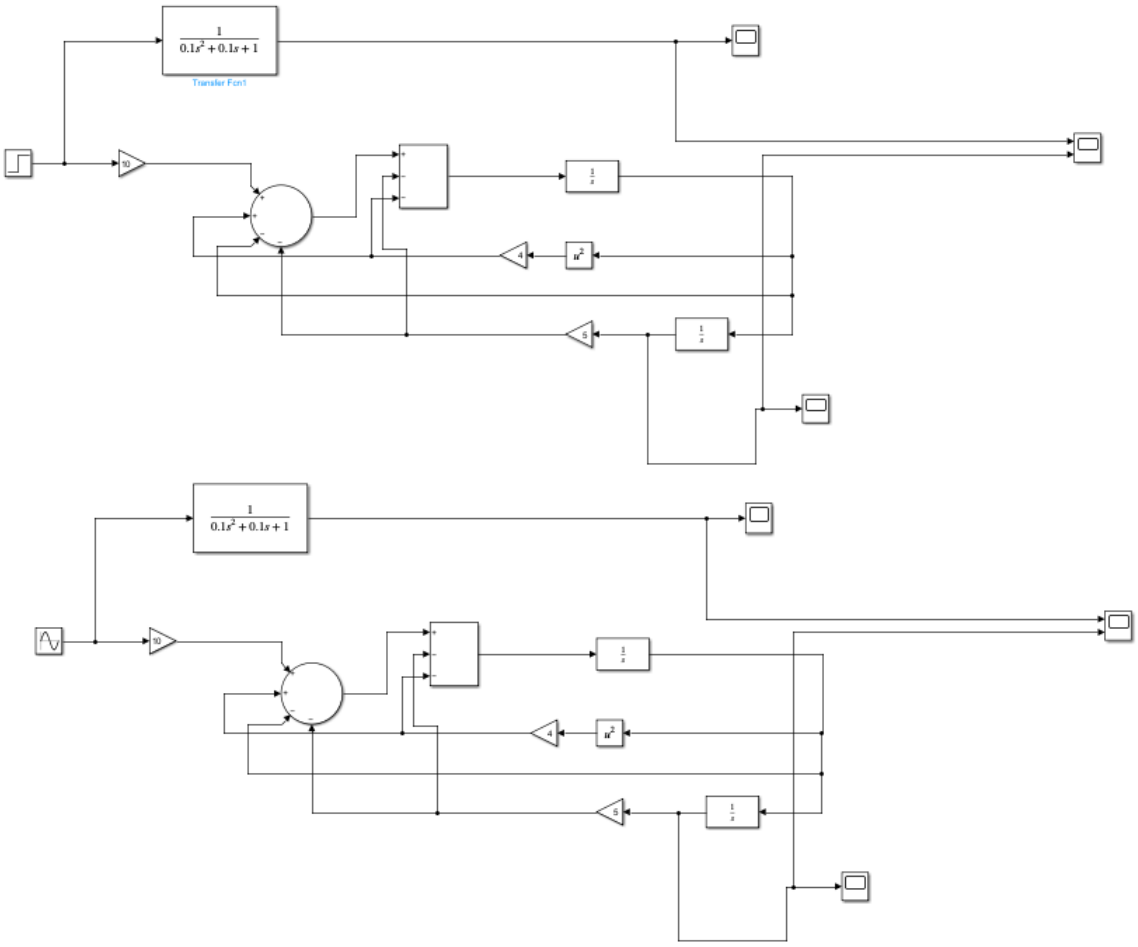

The output for a constant input signal

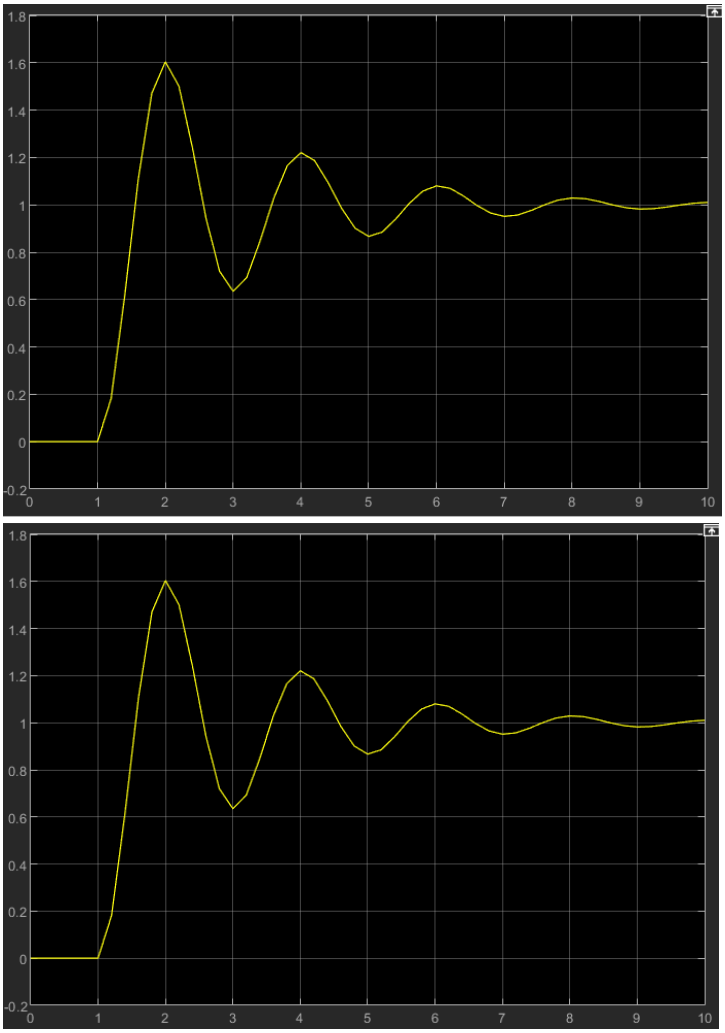

The output for a sine wave input

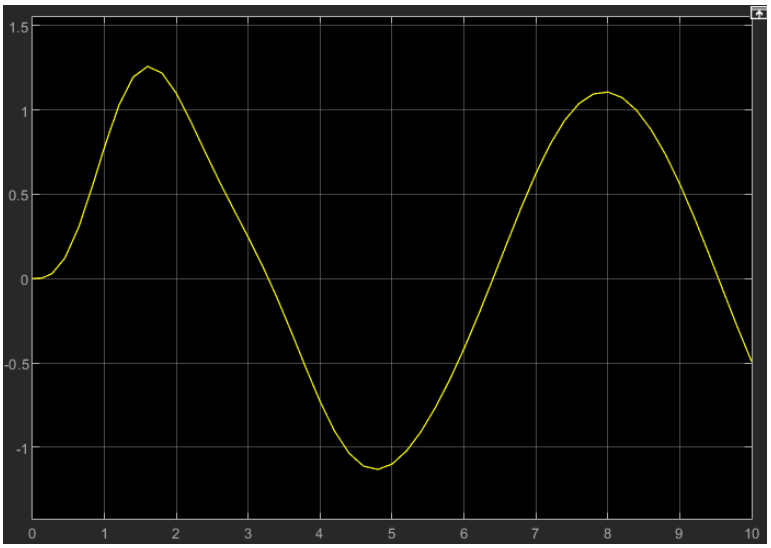

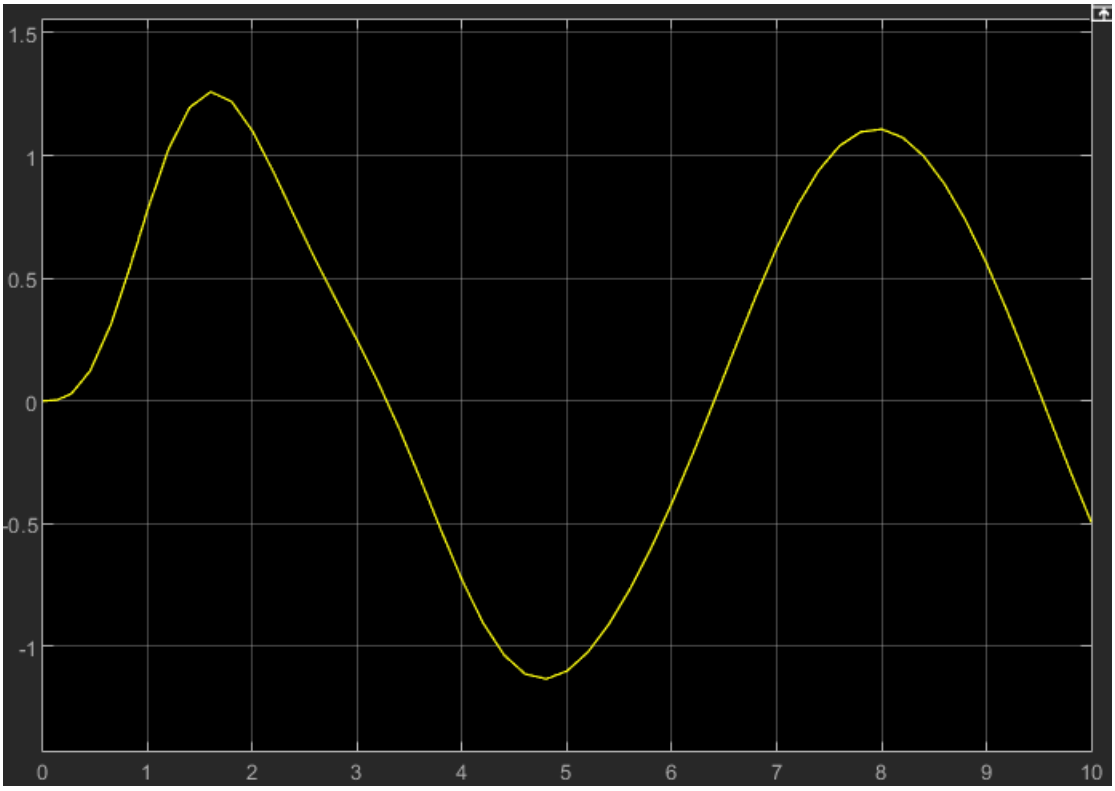

The system behaves like a mass spring system

Question 7

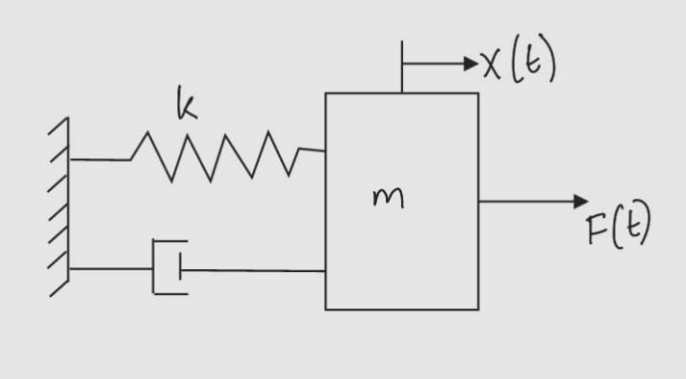

$$f(t) - b\frac{dx}{dt} - Rx = m\frac{d^2x}{dt^2}$$

$$F(s) - bsX(s) - RX(s) = ms^2X(s)$$

$$H(s) = \frac{X(s)}{F(s)} = \frac{1}{ms^2+bs+k}$$

for system 2

$$f(t) = L\frac{di}{dt} + Ri + \frac{1}{C}\int i\,dt$$

$$F(s) = msI(s) + bI(s) + \frac{k}{s}I(s)$$

$$F(s) = I(s)\frac{(ms^2+bs+k)}{s}$$

i, $\frac{dq}{dt}$ $\quad I(s) = sQ(s)$

$$F(s) = \frac{sQ(s)(ms^2+bs+k)}{s}$$

$$\frac{Q(s)}{F(s)} = \frac{1}{ms^2+bs+k}$$

Both systems have the same transfer function

To simulate the mass-spring system using a passive circuit, electrical components are used to symbolize the physical elements of the system. The coil (L) mirrors the system's mass (m) by storing energy in a field akin to the motion-storing mass. Resistance (R) reflects the damping factor (b), as it disperses energy as heat analogous to the damping factor's frictional energy dissipation. Capacitor (C) represents the spring constant (k) since it stores energy in an electric field, similar to the spring constant's potential energy storage. For dynamic system modeling, we utilize Kirchhoff's Voltage Law (KVL). This equation is then Laplace-transformed to yield a transfer function mirroring the Laplace transforms of input and output. Assuming the input as the inductor's voltage and the output as the voltage across the series resistor, capacitor, and inductor, the circuit schematic can be depicted.

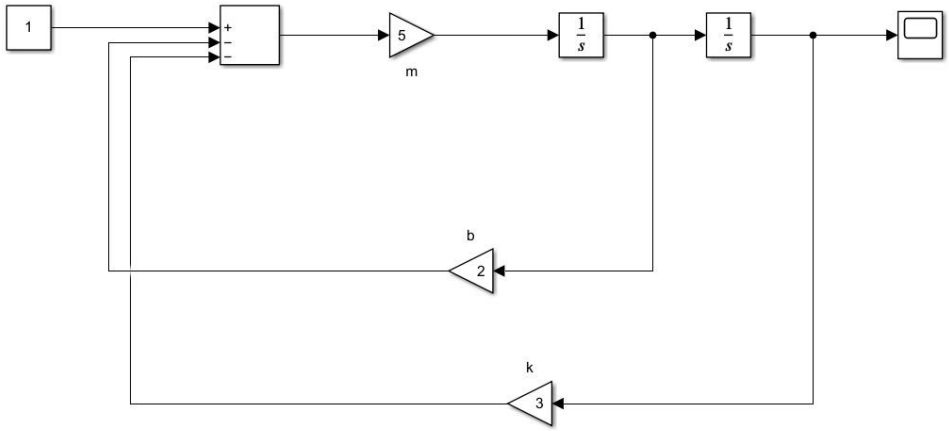

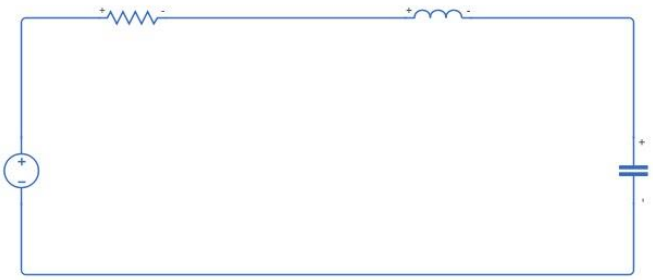

F(s) = (ms^2 + bs + k)X(s)

Question 8

To represent a variable delay as a transfer function in the form of $e^{-sT(t)}$ is incorrect as delay T is not variable as a function of time.
The expression for delay transfer function is e^{-sT}

Laplace transform of a time delayed signal $x(t-T)$

$$X(s) = \int_0^\infty x(t-T)\, e^{-st}\, dt$$

$$v = t - T \Rightarrow t = v + T$$
$$dt = dv$$

$$X(s) = \int_{-T}^{\infty} x(v)\, e^{-s(v+T)}\, dv$$

$$X(s) = e^{-sT} \int_{-T}^{\infty} x(v)\, e^{-sv}\, dv \quad - (1)$$

This integration can not be performed as it gives a math error
Delay function can not be integrated

The integral of equation (1) is the laplace transform of $x(t)$ multiplied by e^{-sT} which gives delay.

$$X(s) = e^{-sT} Xd(s)$$

$Xd(s)$ is a laplace transform of delayed i/p signal $X(t-T)$

The transfer function for the delay is independent of time.
∴ It is incorrect to represent variable delay as a transfer function as 'T' is a constant and not a variable time function

Question 9

In communication systems, there's often a delay between the transmission and reception of signals. This delay arises from various factors like distance, processing duration, and propagation time. The Pade approximation is utilized to estimate a function, often expressed as a ratio of two polynomials that simplifies the analysis and design of communication systems.

The process of Pade approximation for communication time delay involves determining a rational function that closely represents the delay function across a specific frequency spectrum. Typically, this rational function takes the form: $$D(s) = \frac{(b_0+b_1 s+b_2 s^2+\ldots+b_m s^m)}{(1+a_1 s+a_2 s^2+\ldots+a_n s^n)}$$

Here, 's' signifies the Laplace-transformed variable, 'm' and 'n' are positive integers, and coefficients such as b_0, $b_1 \ldots b_n$; a_0, $a_1 \ldots a_n$ are determined by aligning the coefficients of the numerator and denominator polynomials with those of the reference function.

The derived Pade approximation proves valuable for the analysis and design of communication systems affected by latency, including control systems, signal processing systems, and network communication systems.

```
% Bode plots - Pade approximations
figure()
hold on
delay = 0.1; %100ms
% First order approximation
[numerator1, denominator1] = pade(delay,1); % time delay of 0.2 seconds
sys1 = tf(numerator1, denominator1);
bode(sys1)


% Second order approximation
[numerator2, denominator2] = pade(delay,2);
sys2 = tf(numerator2, denominator2);
bode(sys2)

% Third order approximation
[numerator3, denominator3] = pade(delay,3);
sys3 = tf(numerator3, denominator3);
bode(sys3)

legend('1st Order Pade approximation', '2nd Order Pade approximation', '3rd Order Pade approximation')
hold off
```

```
sys1 =

  -s + 20
  -------
  s + 20

Continuous-time transfer function.
Model Properties

sys2 =

  s^2 - 60 s + 1200
  -----------------
  s^2 + 60 s + 1200

Continuous-time transfer function.
Model Properties

sys3 =

  -s^3 + 120 s^2 - 6000 s + 1.2e05
  --------------------------------
  s^3 + 120 s^2 + 6000 s + 1.2e05

Continuous-time transfer function.
Model Properties
```

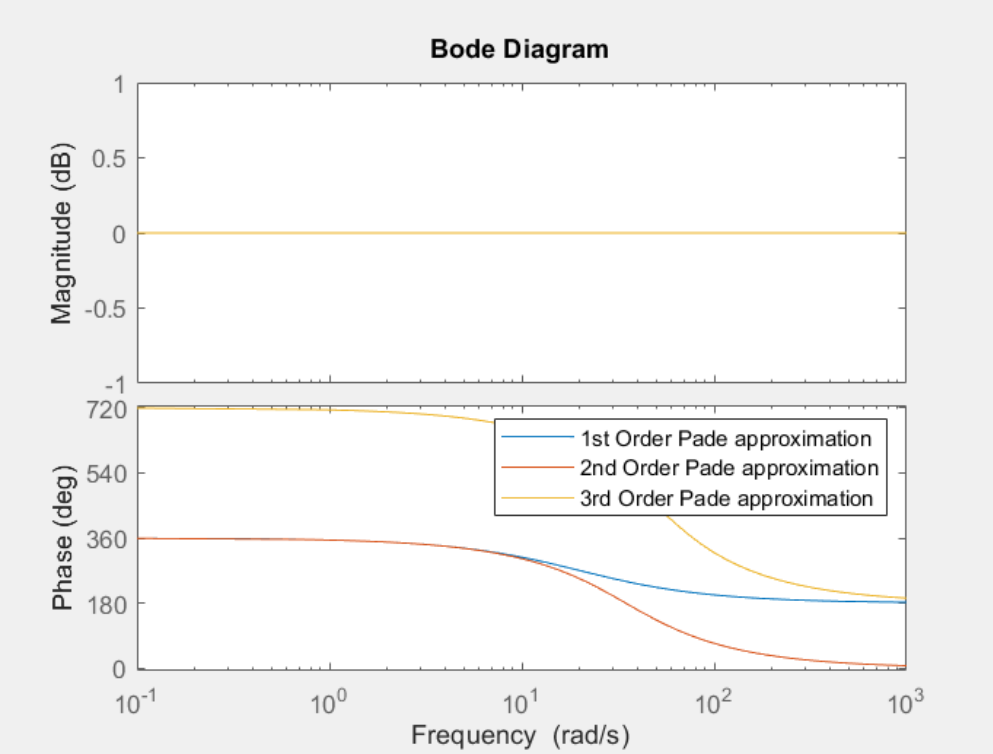

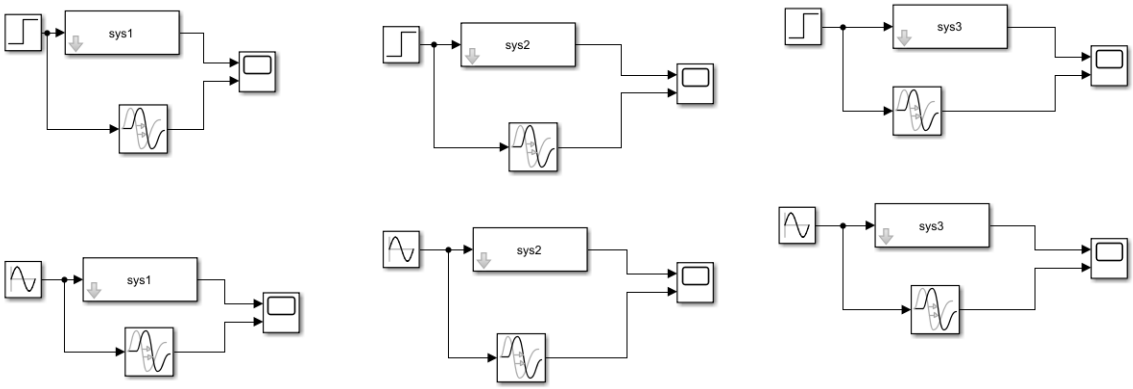

Sys 1 step function -

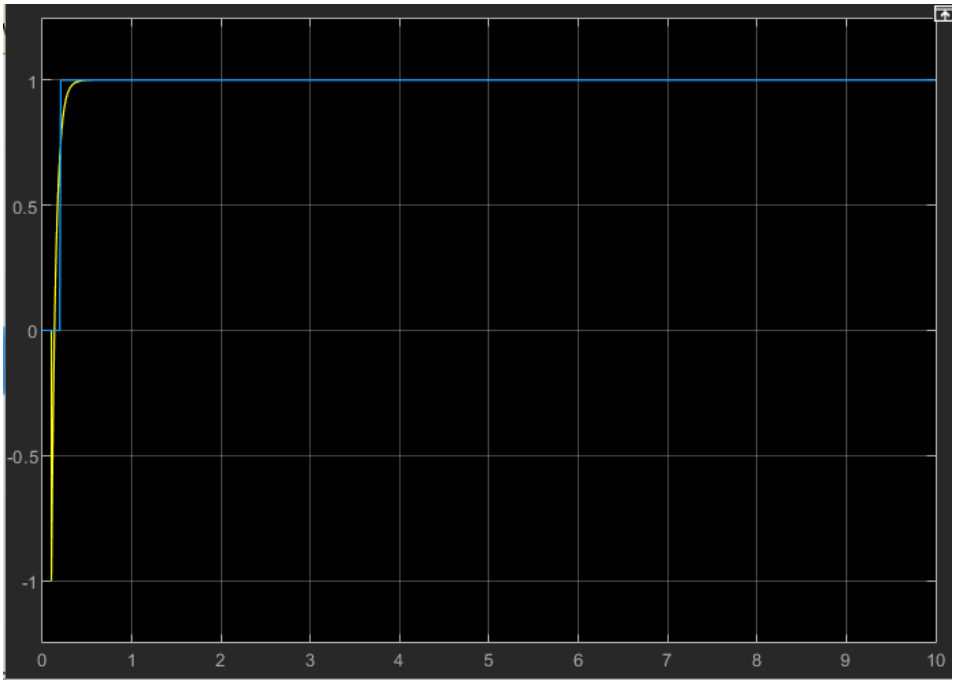

Sys 1 sine function -

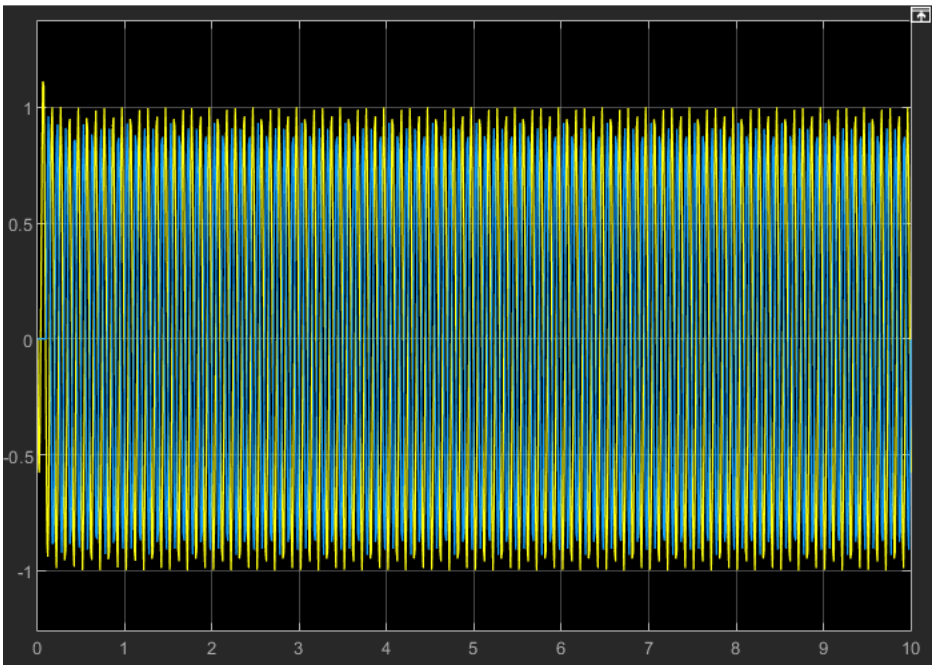

Sys 2 step function -

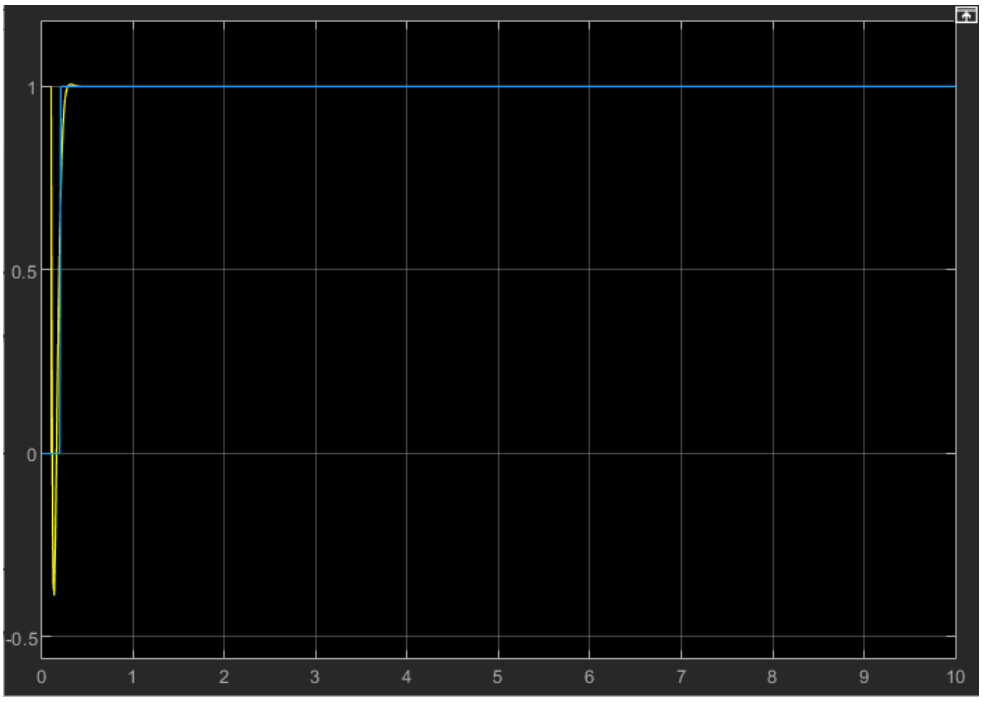

Sys 2 sine function -

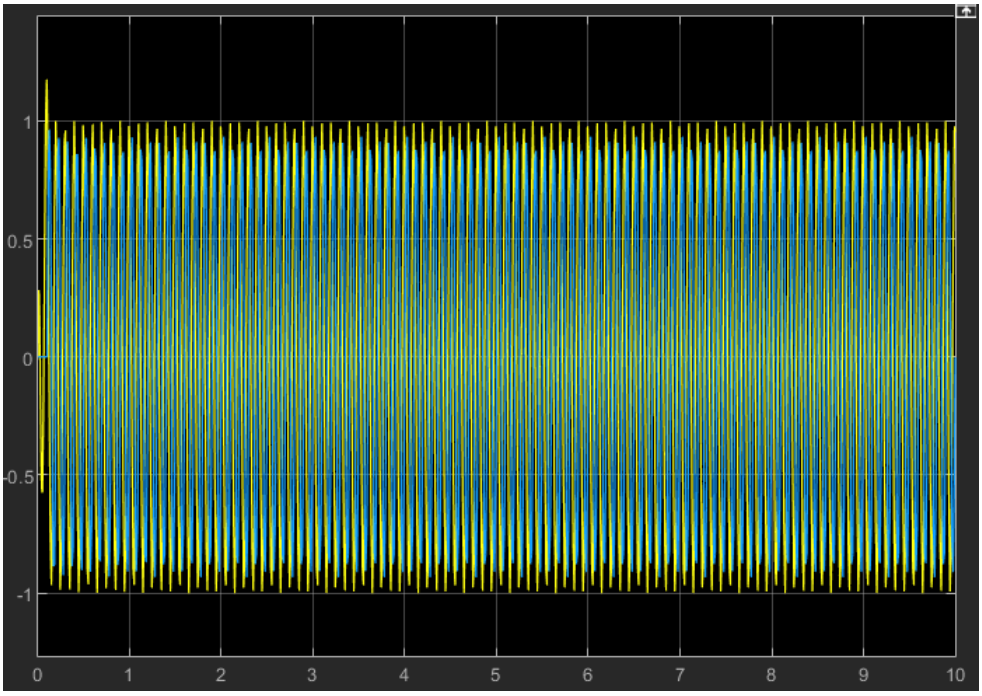

Sys 1 step function -

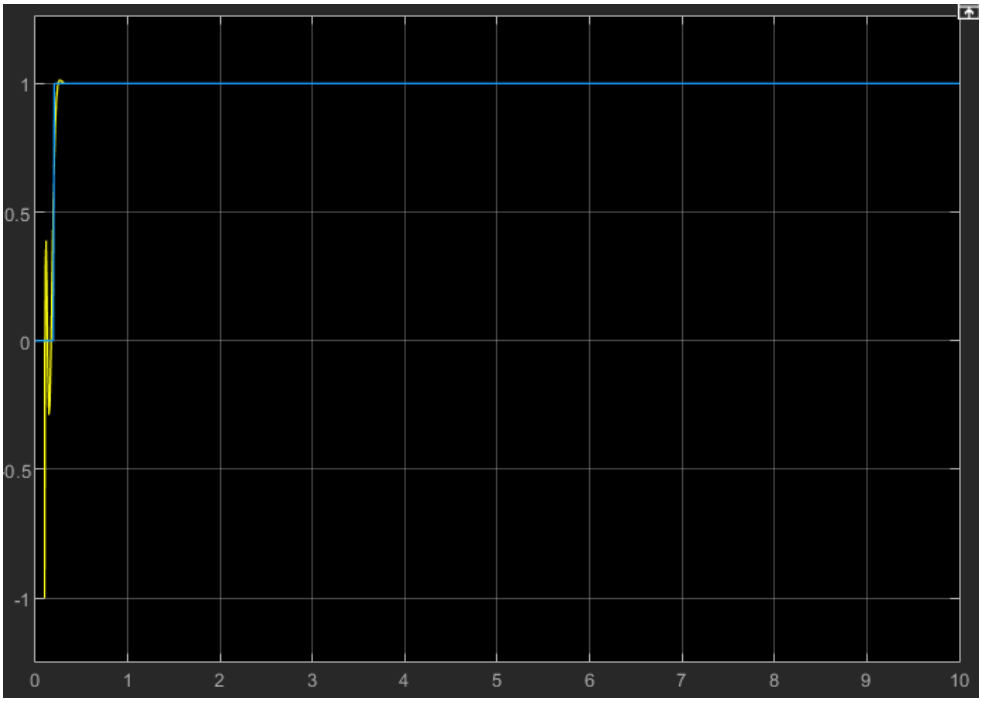

Sys 1 step function -

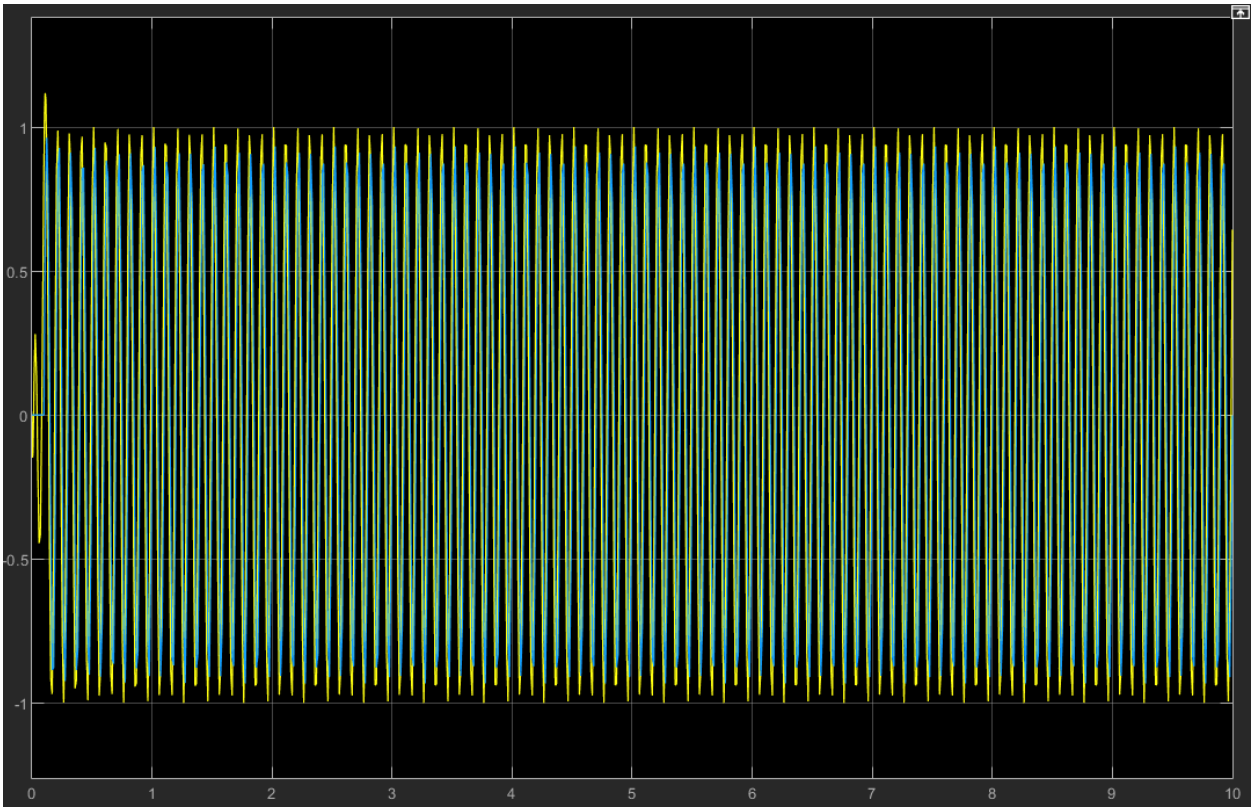

Question 10

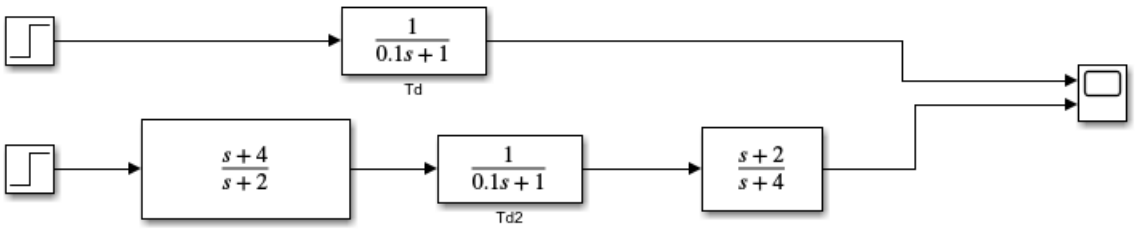

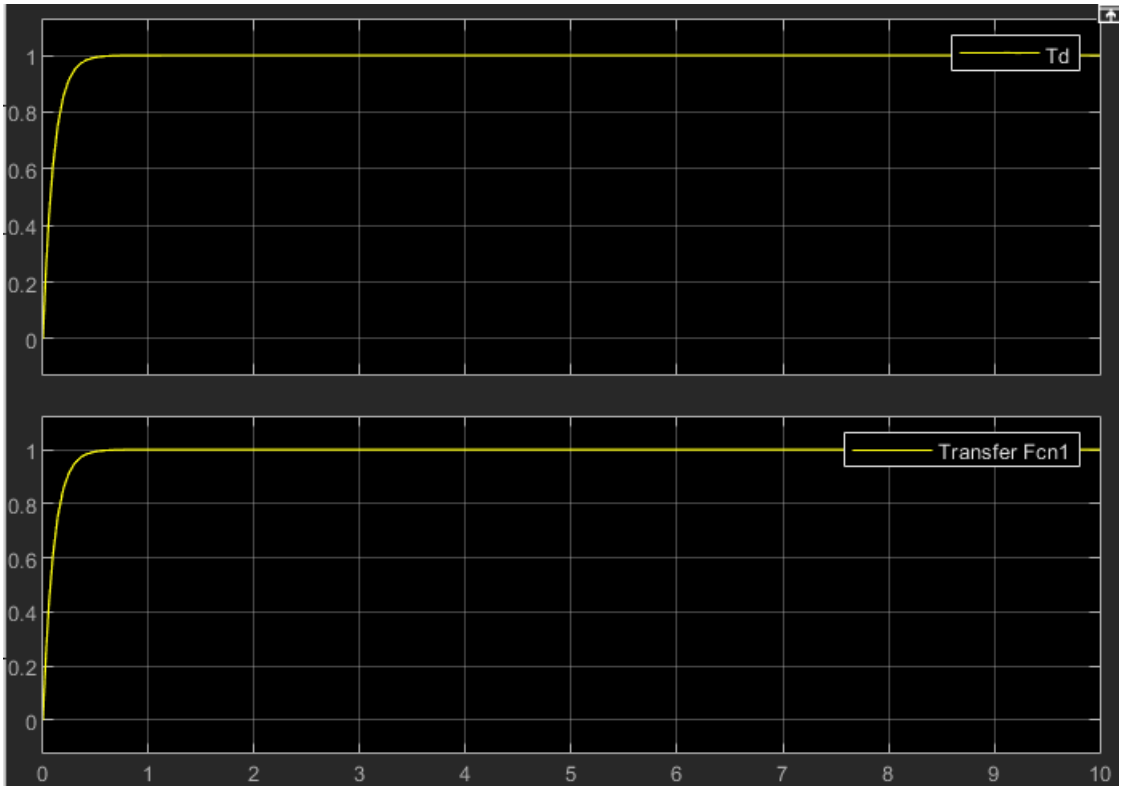

From the above graph, zero pole cancellation result in desired behavior

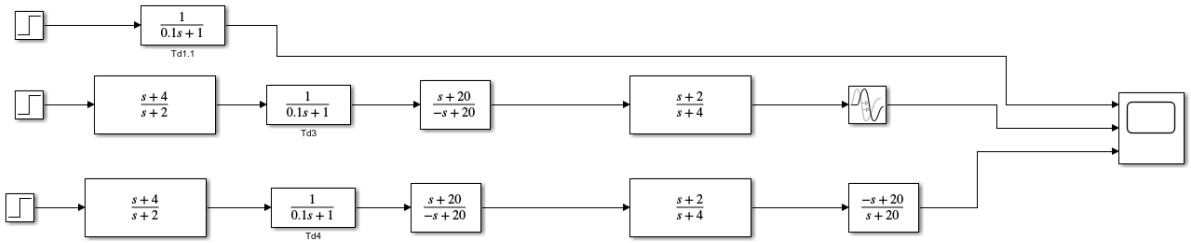

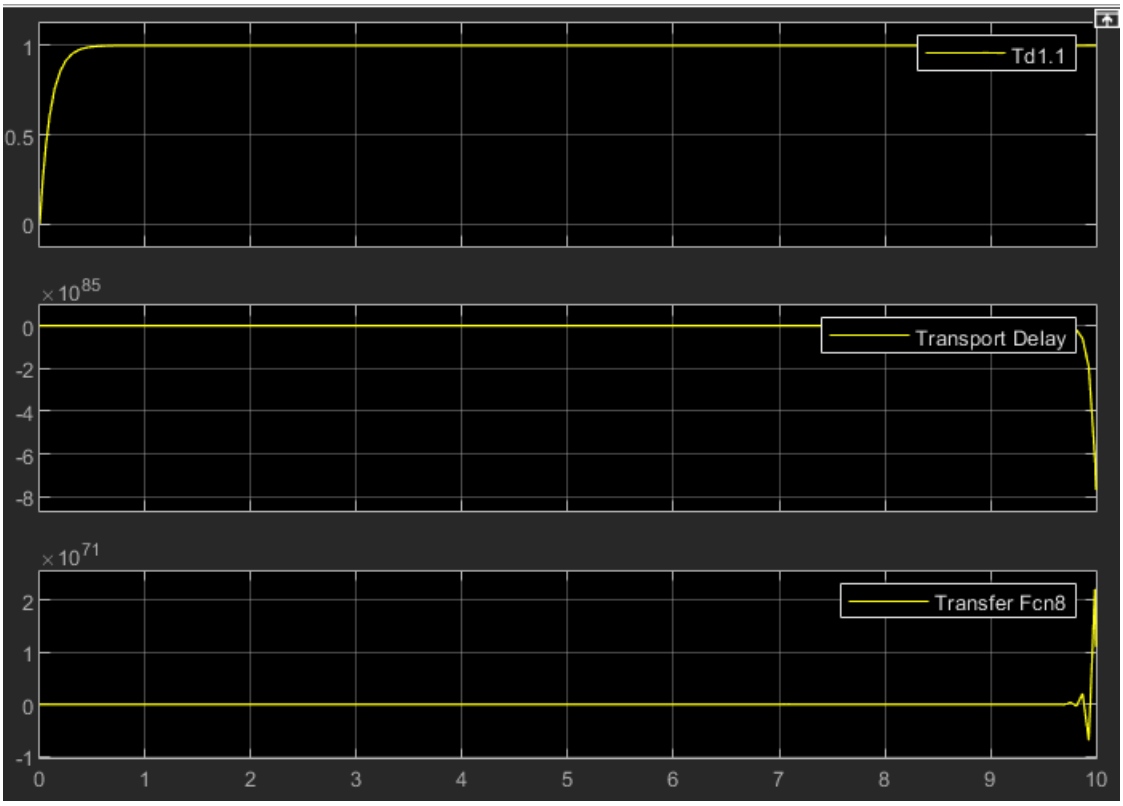

$$T_f = \frac{S+2}{S+4}$$

$$T_d = T_c + T_f \qquad T_d = \frac{1}{0.1S+1}$$

New Transfer function with delay

$$T_{f_2} = \frac{S+2}{S+4} e^{-ST}$$

$$T_c = \frac{S+4}{S+2} \times \frac{S+20}{-S+20} \times \frac{1}{0.1S+1} \times \frac{S+2}{S+4} \times \frac{-S+20}{S+20}$$

$$T_c = \frac{1}{0.1S+1}$$

Question 11

- The Bode plot of the first function illustrates the response of the initial transfer function, characterized as a first-order low-pass filter with a magnitude at low frequency close to 0 dB, suggesting a gain of 1. The magnitude starts to increase gradually, indicating some amplification of the signal as the frequency increases. The magnitude starts to decrease at a higher rate suggesting the system becomes more attenuating for high-frequency signals. The phase starts at -90 degrees for low frequencies, rises to 0 degrees at the cut-off frequency, and remains consistent thereafter.
- The Bode plot of the second function illustrates the response of the initial transfer function, characterized as a first-order high-pass filter with magnitude, at low frequencies the magnitude is close to 0dB. This indicates that the system has a gain of 1 at low frequencies, the signal passes through the system without significant attenuation. As the frequency increases, the magnitude starts to increase and the signal is being amplified. The rate of increase is 20 dB per decade, which corresponds to a slope of 1 in the Bode plot. This is the cutoff frequency is 1Hz Frequencies lower than the cutoff frequency is passed with little attenuation, while frequencies higher than the cutoff frequency are amplified. After the peak, the magnitude starts to decrease at a rate of 20 dB per decade (slope of -1). This indicates that the system is acting like a low-pass filter for high frequencies. The phase curve of this transfer function is -90 degrees at low frequencies and increases to 0 degrees at the peak frequency and then continues to increase by 90 degrees per decade.
- The Bode plot of the first function illustrates the response of the initial transfer function, characterized as a band pass filter with the magnitude at low frequencies close to 0 dB, suggesting a gain of 1. This means low-frequency signals pass through the system with little to no change in magnitude. The magnitude starts to increase gradually, indicating some amplification of the signal as the frequency increases. The magnitude starts to decrease at a higher rate suggesting the system becomes more attenuating for high-frequency signals. The phase curve of this transfer function is -90 degrees at low frequencies and increases to 0 degrees at the peak frequency and then continues to increase by 90 degrees per decade. the magnitude is close to 0 dB, suggesting a gain of 1.

```
% Define the transfer functions
numerator_1 = 1;
denominator_1 = [0.2, 1];
sys_1 = tf(numerator_1, denominator_1);
figure;
bode(sys_1);
title('Bode Plot of Transfer Function 1');

numerator_2 = [1, 0.1]
denominator_2 = [0.2, 1];
sys_2 = tf(numerator_2, denominator_2);
figure;
bode(sys_2);
title('Bode Plot of Transfer Function 2');

numerator_3 = [1, -0.1]
denominator_3 = [0.2, 1];
sys_3 = tf(numerator_3, denominator_3);
figure;
bode(sys_3);
title('Bode Plot of Transfer Function 3');
```

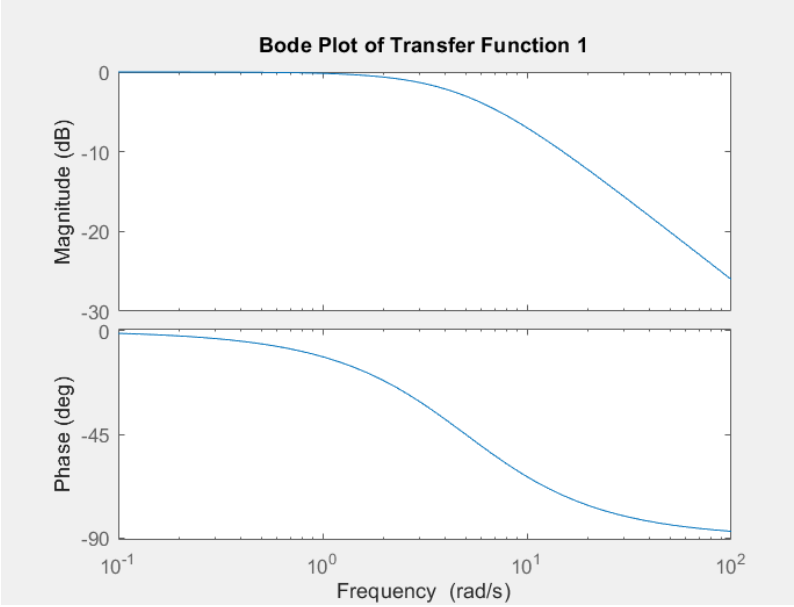

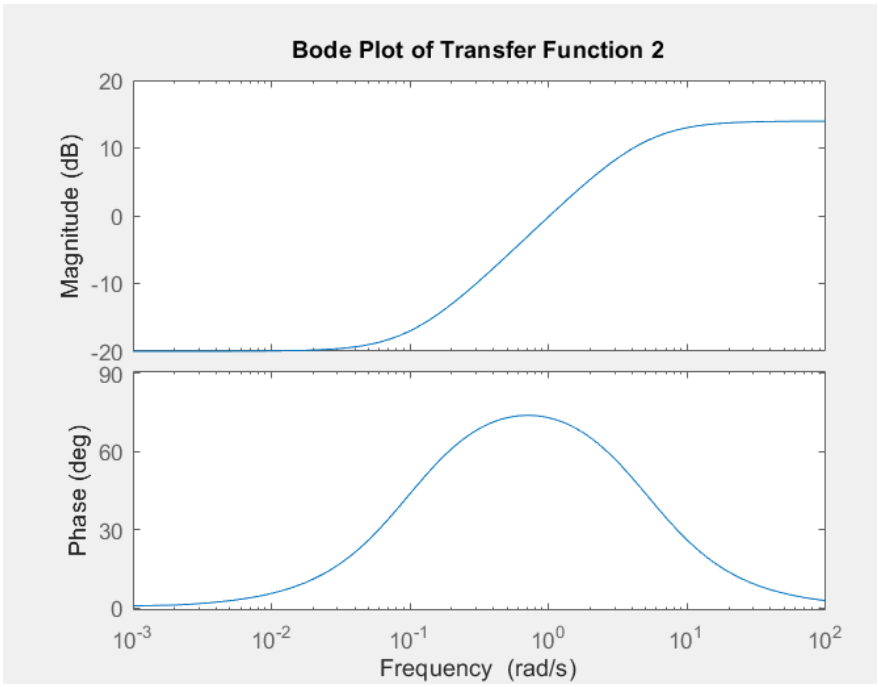
Bode Plot of Transfer Function 2
Magnitude (dB)
20
10
0
-10
-20
Phase (deg)
90
60
30
0
10^{-3}
10^{-2}
10^{-1}
10^{0}
10^{1}
10^{2}
Frequency (rad/s)

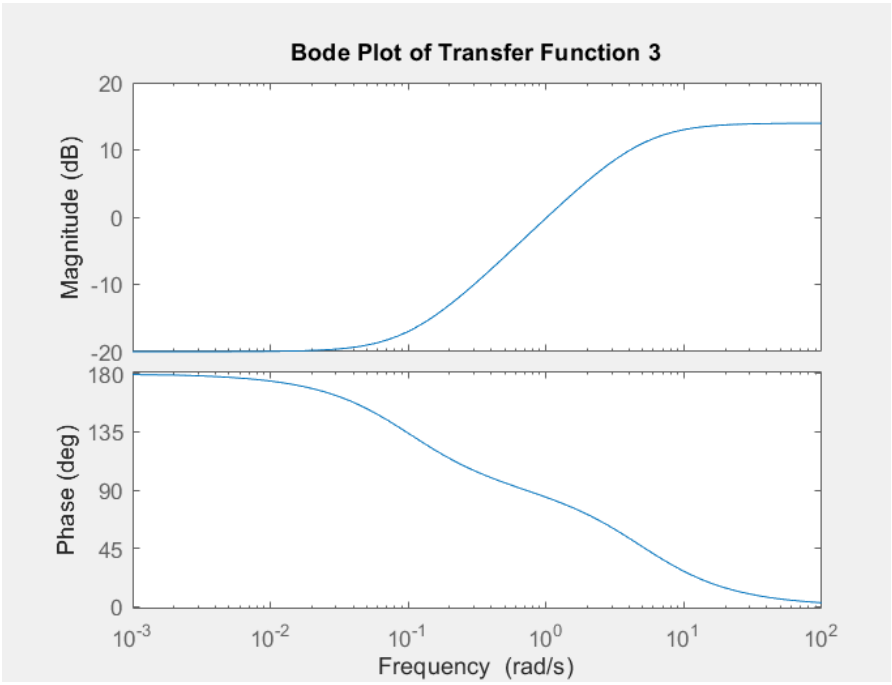
Bode Plot of Transfer Function 3
Magnitude (dB)
20
10
0
-10
-20
Phase (deg)
180
135
90
45
0
10^{-3}
10^{-2}
10^{-1}
10^{0}
10^{1}
10^{2}
Frequency (rad/s)

Question 12

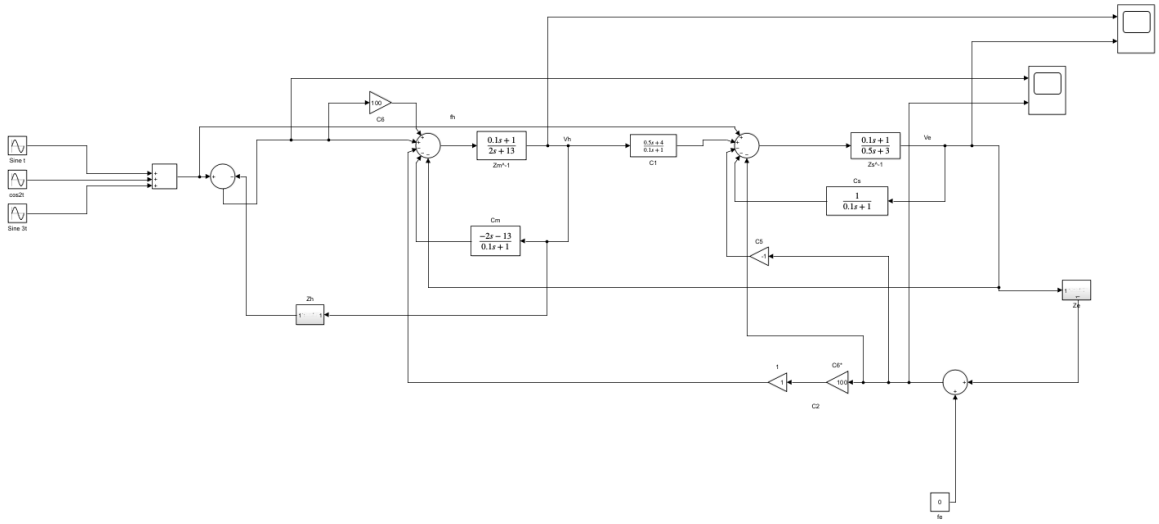

There is no time delay in the system and it is a transparent system. Z_{to} = Z_e.

It is observed that V_e imitates the speed of the leader V_h, while the force exerted by the environment F_e exactly equals the force of the human operator F_h indicating that the system achieves flawless speed and force tracking, the system has no latency and its perceived impedance (Z_e) equals the impedance of the surrounding environment (Z_{to}), the system is fully transparent and achieves 100% accuracy and no time delay.

Force and velocity Graphs

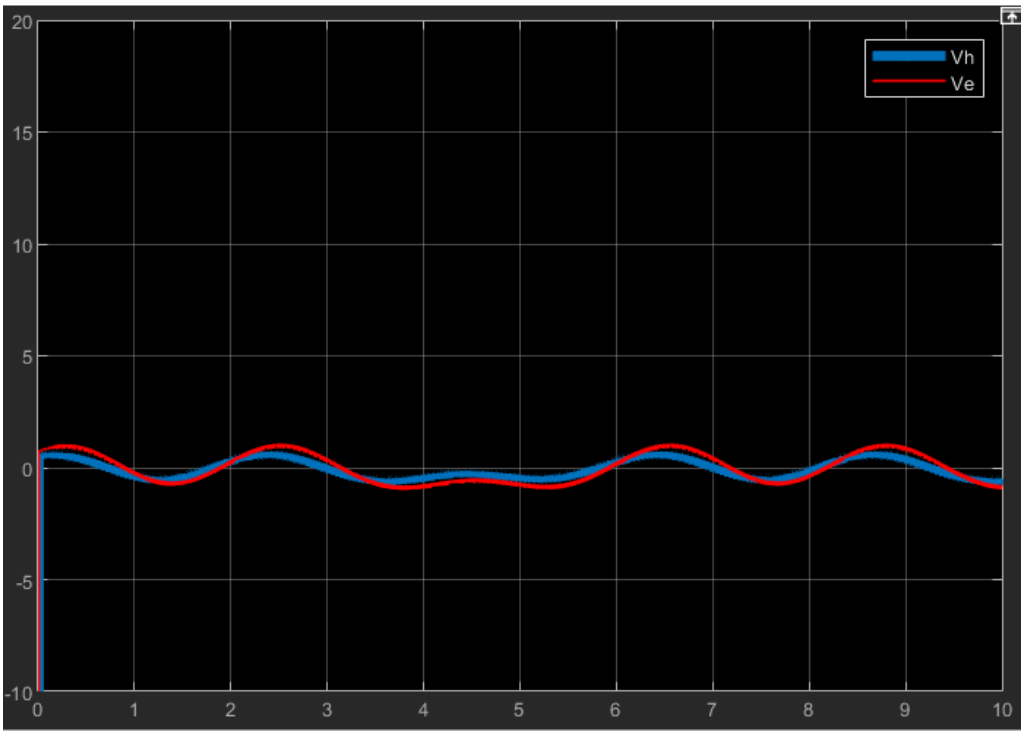

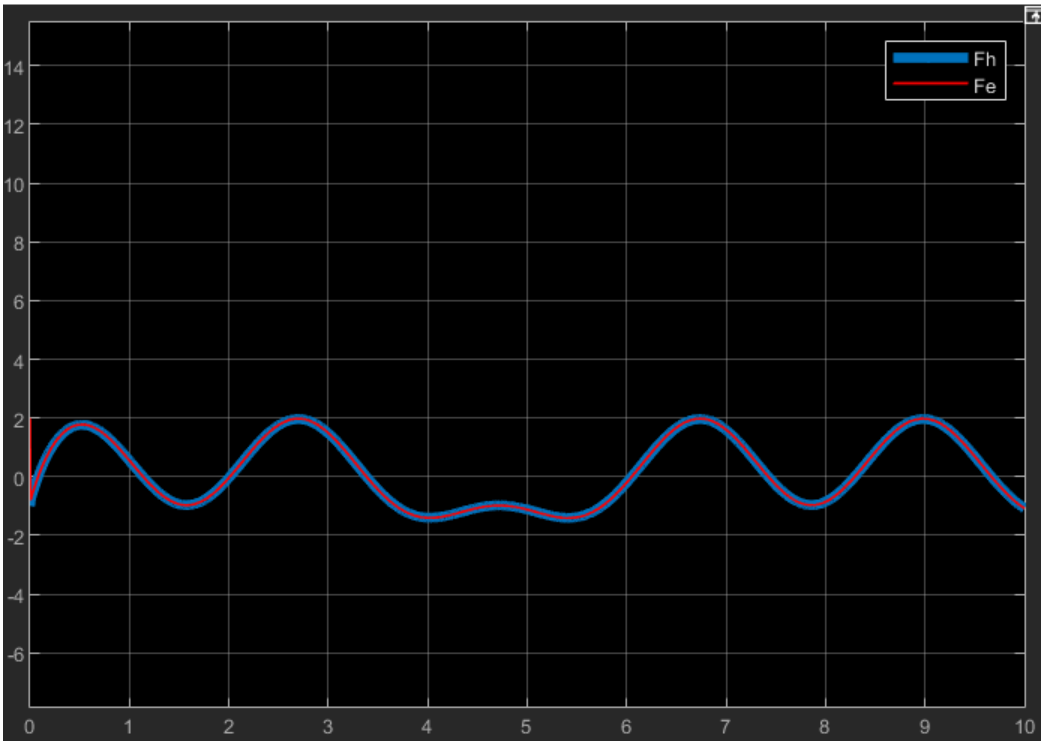
Fh
Fe
14
12
10
8
6
4
2
0
-2
-4
-6
0
1
2
3
4
5
6
7
8
9
10